A New Test Method for High-Temperature Fracture of Alloys and Some Corresponding Results

Shaoqin Zhang[1,2,*], Wanlin Guo[2,*], He Li[1], Huihua Zhang[1], Ying Deng[1], Qiong Wu[1], Qinghui Xiao[1], Peng Zhou[1]

[1] Key Laboratory of Nondestructive Testing, Ministry of Education, Nanchang HangKong University, Nanchang 330063, China
[2] State Key Laboratory of Mechanics and Control of Mechanical Structures, Nanjing University of Aeronautics and Astronautics, Nanjing 210016, China
* Corresponding author: shaoqinzhangniat@yahoo.com.cn, wlguo@nuaa.edu.cn

Abstract A moiré interferometry-based experimental method is first introduced for high-temperature, mixed-mode fracture testing. The method allows real-time observation of surface deformation of cracked specimens and crack-tip plastic zone at elevated temperatures. Based on the moiré fringe patterns captured real time through image acquisition system, important fracture parameters, such as the crack open displacement, the crack initiation load, the ultimate load, etc., can be determined. With these data, the stress intensity factor, load bearing capacity, fracture ductility, strain, and stress fields near the crack-tip can be obtained. The method has been successfully applied to investigate pure mode I, I-II mixed-mode fracture performance of high temperature alloys. Furthermore, some significant thickness effects achieved by the group of researchers on the mixed-mode fracture performance of TC11 titanium alloy at high temperatures are cited and briefly introduced. Finally, three dimensional finite element simulations are performed for the tensile-shearing specimens at an elevated temperature. Simulation results are in agreement with measurements.

Keywords Moiré interferometry, High temperature, Mixed mode fracture, Thickness effect

1. Introduction

In industrial fields, such as aerospace, petrochemical, and dynamic transportation, there is a growing demand for high-temperature structural materials. The rising demand makes the issues of reliability design, failure analysis, and safety evaluation for high-temperature structures increasingly important [1-5]. The performance of engineering materials, especially metal materials, is always sensitive to temperature. At an elevated temperature, internal molecular motion aggravating, phase changing, cavity and micro crack emerging in materials make their fracture property significantly different from that at room temperature [3]. With the field of fracture still in development, high-temperature behavior remains one of the unresolved fundamental issues [6]. A better understanding of the fracture behavior is important. High-temperature components, such as engine turbine and blade, steam boiler and pipeline, and steam turbine bear complex loading at high temperatures. Therefore, mixed-mode fracture testing of materials from room to high temperature is necessary.

By far, the research on two-dimensional (2D) cracks of single and mixed modes under room temperature (RT) becomes better and approaches perfection day by day. However, most of the previously conducted analytical and numerical investigations in fracture mechanics were focused on 2D or axisymmetric geometries, although three-dimensional (3D) effects were often acknowledged. The stress state near an actual crack tip is always 3D, and the meaning of the results obtained within the 2D theories and their relation to the actual 3D stress distribution is still not fully understood [7].

3D effects increasingly drew attention in recent years from material experiments in laboratories to the real structure [6-8]. Experiments have shown that some damages or failure characteristic quantities, which are regarded as material constants, indeed are related to the structural geometry [5]. A large number of theoretical analysis, experimental investigations, and numerical computations reveal significant 3D effects such, as the thickness effect [9-14]. 3D fracture theory, founded in consideration both of in-plane and out-plane constraints, has made important progress [15-18]. The research on mixed-mode cracks gradually progresses from the 2D hypothesis to the 3D assumption [19-21]. Comparatively, research mainly focuses on the cracks of ideal mode I, 2D problems, theoretical analysis, and numerical computations. Experimental investigations, especially observations and measurements of real 3D fracture of mixed-mode cracks under high temperature, are very limited. There is no complete analytic solution for 3D fracture problems due to mathematical difficulties. Research on 3D fracture problem of mixed-mode cracks under high temperature still needs to be done. The existing theoretical fracture models have many weaknesses and are not verified by experiment and practical use [5]. In a conceptual paper on the past and future development of fracture mechanics, Erdogan [6] identifies 3D effects, high-temperature behaviors, computational methods, and experimental methods as the areas where further intensive research is needed.

A new fracture experimental technique based on the moiré interferometry is introduced in this study, by which I-II mixed-mode fracture phenomenon could be surveyed and recorded when temperature is high (say at least several hundreds of degrees in Celsius). Finite through-thickness cracked specimens are employed in tests under the coupling of thermal environment and mixed-mode loading. Displacement field moiré fringes around the crack are recorded. This experimental method was successfully used in investigation of fracture properties of high-temperature alloys. Several specific thickness effects at high temperatures are revealed based on the experimental results.

2. High-temperature, mixed-mode fracture test

2.1. Experimental setup and procedures

High-temperature moiré interferometry system has been successfully used in investigation of crack growth of pure mode I [22-24]. The same is employed in this present mixed-mode fracture research. The tensile-shearing specimen dimensions and mixed-mode loading fixture are given in Ref. [25]. A special orthogonal diffraction grating with high temperature resistance is chosen and fabricated on a highly polished surface of a specimen by photoetching and chemical etching [26]. Two sets of grid lines of the orthogonal grating are parallel to and perpendicular to the crack, respectively. A rotatable U-V mirror set [27] is invented for the purpose of the mixed-mode fracture experiment. The mirror set is designed to rotate by the same angle when angle β existed between loading direction and crack perpendicular, as shown in Figure 1. Consequently, the displacements normal to the crack (Mode I) and parallel to the crack (Mode II) were effectively separated, ensuring that moiré fringes corresponding to the u-displacement and v-displacement always are parallel and perpendicular to the crack at any I-II mixed-mode loading. The fracture testing procedure based on moiré interferometry at elevated temperature, including preparations of specimens, fabrication of specimen grating, heating, maintenance of temperature, and loading until fracture, is detailed in Ref.

[25].

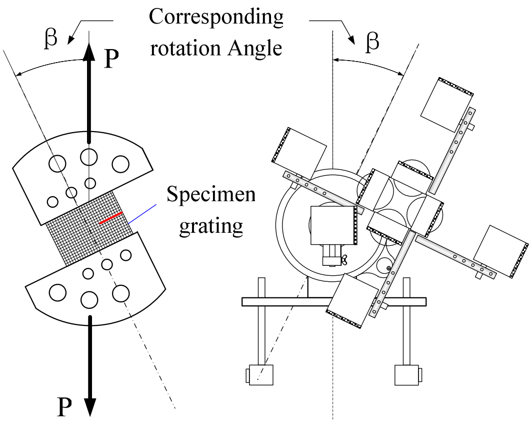

Figure 1: Mixed-mode fracture test fixture and corresponding arrangement of U-V mirror set

2.2. Evaluation of fracture parameters

Typical moiré fringes seen during the test are illustrated in Figure 2. The fringes tend to be closer to each other and move towards the crack tip with the load. Once the load increases, a small dark spot appears around the crack tip on the surface. This means a plastic zone forms and develops as the load increases. The crack mouth open displacement (COD), which is the relative displacement of point A and B in Figure 2, is measured using a v-displacement field moiré fringes based on the principle of moiré interferometry. Special image processing techniques, such as smoothing, filtering, and refining, are used to reproduce the moiré fringe for counting the number of fringes and reproducing the profile of plastic zone. The stress intensity factors K_I, K_{II}, K_{eff} are determined based on load, loading angle, and crack length when the fracture test is finished [25]. Load-COD curves and K_{eff}-COD curves then can be drawn.

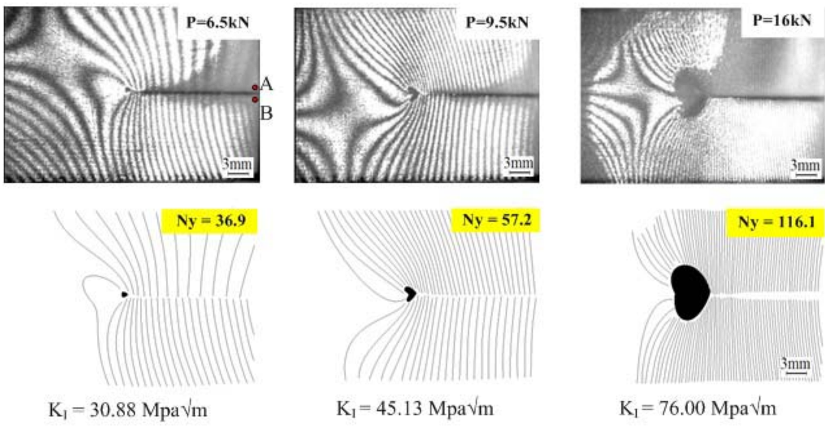

Figure 2: Representative moiré fringe patterns during the test and reproduced images

2.3. Measurement of crack initiation angle

From 2D fracture mechanics, the crack initiation angle is usually defined as the included angle between the initiation orientation and the original crack orientation at half-thickness (middle) plane. The included angle is the one between the flat region B and the pre-cracked plane A in Figure 3. It is an important parameter for mixed-mode fracture but is often difficult to measure. To obtain the angle, as a common methodology, the specimen is first cut into two separate parts from the middle plane, and then the angle is measured [19]. However, it does not work well for metallic material and thin samples. The following method is employed to measure the initiation angle. First, a CCD camera is used to take photographs of the profile of the fractured specimens, as shown in Figure 3 (c). Subsequently, the profile photographs are processed as computer image files. The most important step in this procedure is accurately determining and drawing the tangent line at the beginning of the crack growth path at the middle thickness and the pre-crack line. Finally, the initiation angle is obtained by measuring the angle between the two lines. Based on the above mentioned scheme, the initiation angle of the specimen in Figure 3 is 27.7°. Using the same method, the included angle between the pre-cracked plane and the pre-notched plane (e.g., 5.5° in Figure 3(c)), which is the machining error and which should be distinguished from the initiation angle, also can be recorded.

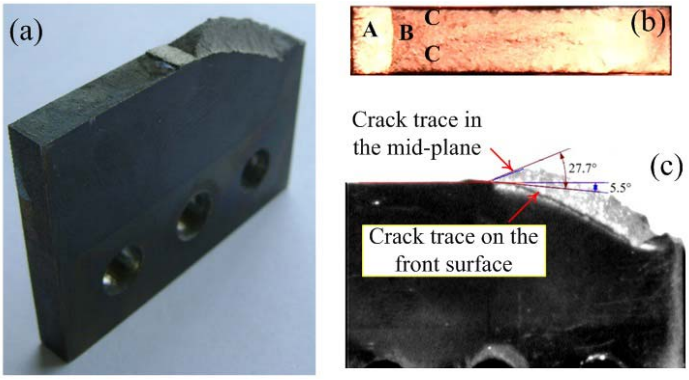

Figure 3: Representative macro pictures of the fracture surface with characteristic regions. A is the fatigue pre-crack, B is the flat fracture region, and C is the shear lip.

3. Fracture test on TC11 titanium alloy material

Mixed-mode fracture experiments are conducted on TC11 titanium alloy specimens with varied thicknesses at RT and elevated temperature. The experiments are conducted using the newly developed testing technology, which is based on high-temperature moiré interferometry. Some results are very unusual and remarkable.

3.1. Experimental results at elevated temperature [25]

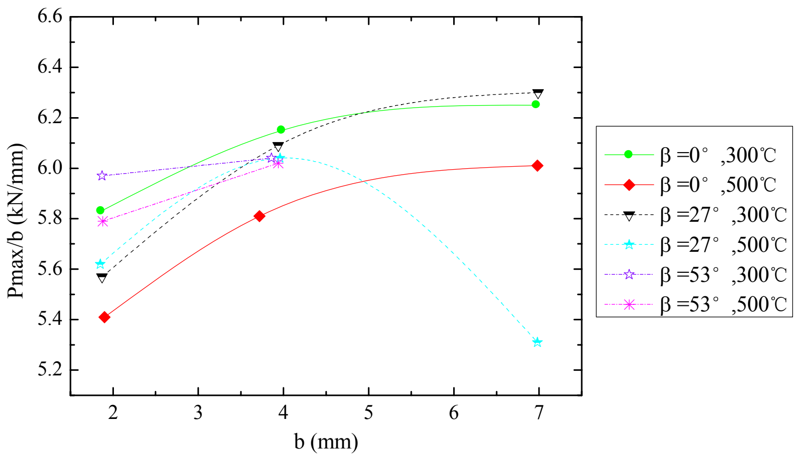

Figure 4: Load capacity versus thickness b and loading angles β at high temperatures (reproduced from Ref. [25])

Figure 4 illustrates the average results for the specimens in the same thickness group at an elevated temperature. It shows that in addition to some individual cases, the loading capacity increases with the specimen thickness. This observation is contrary to common knowledge. Increasing temperature enhances the fracture load capacity for thick specimens, but reduces it for thin specimens. Detailed analysis is given in Ref. [25]. When fracture toughness is examined, K_{effi} (the stress intensity factor corresponding to the crack initiation load P_{i}) with loading angle β and specimen thickness b appears at high temperatures, as shown in Figure 5. Effects of thickness existed in K_{effi}, although regularity is not obvious. These results again confirm the complex coupled effects of thickness and temperature in the mixed-mode fracture of the alloy.

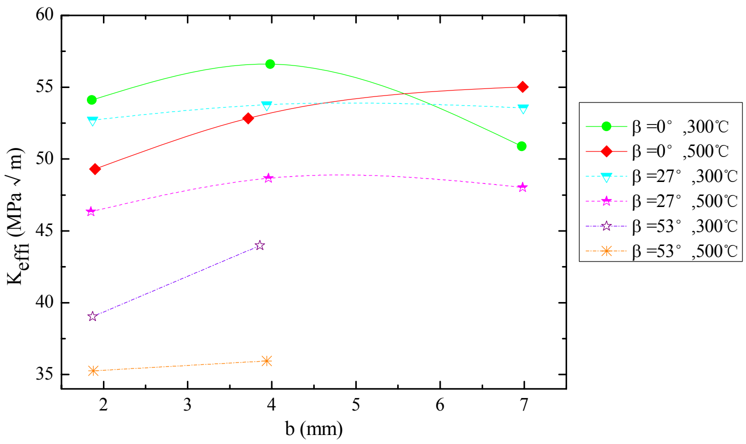

Figure 5: Results of K_{effi} versus thickness b and loading angles β at high temperatures (reproduced from Ref. [25])

The thickness effect is significantly coupled with the temperature effect in mixed-mode fracture of TC11 alloy, which is important for the development of 3D fracture theory under complex loading and temperature conditions. Why did this happen? Is this the peculiarity of titanium alloy or is this a shared property of metals or alloys? To answer the questions, further studies on fracture mechanism of high-temperature fracture should be conducted.

3.2. Qualitative comparison with finite element data

To compare the test results with the numerical solutions, specimens with the same dimensions as in the experiment are modeled using the finite element (FE) software ANSYS. In the 3D simulation, the Ramberg-Osgood constitutive relation [28] is adopted to represent the material nonlinearity. The corresponding parameters are determined through fitting of experimental data. Accordingly, the stress-strain relation is expressed as

$$\varepsilon = \frac{\sigma}{120000} + 9.9879\times10^{38}\left(\frac{\sigma}{120000}\right)^{19.9578} \tag{1}$$

at RT, and

$$\varepsilon = \frac{\sigma}{98000} + 9.089\times10^{11}\left(\frac{\sigma}{98000}\right)^{6.6095} \tag{2}$$

at 500℃.

The contours of Mises stress on the front surface at 500℃ are plotted in Figure 6, where the domain bounded by red lines conforms to the visual region of moiré fringe. In Figure 7, moiré fringe of the same specimen from the tests also is presented. In the first row of Figures 6 and 7, the same load is

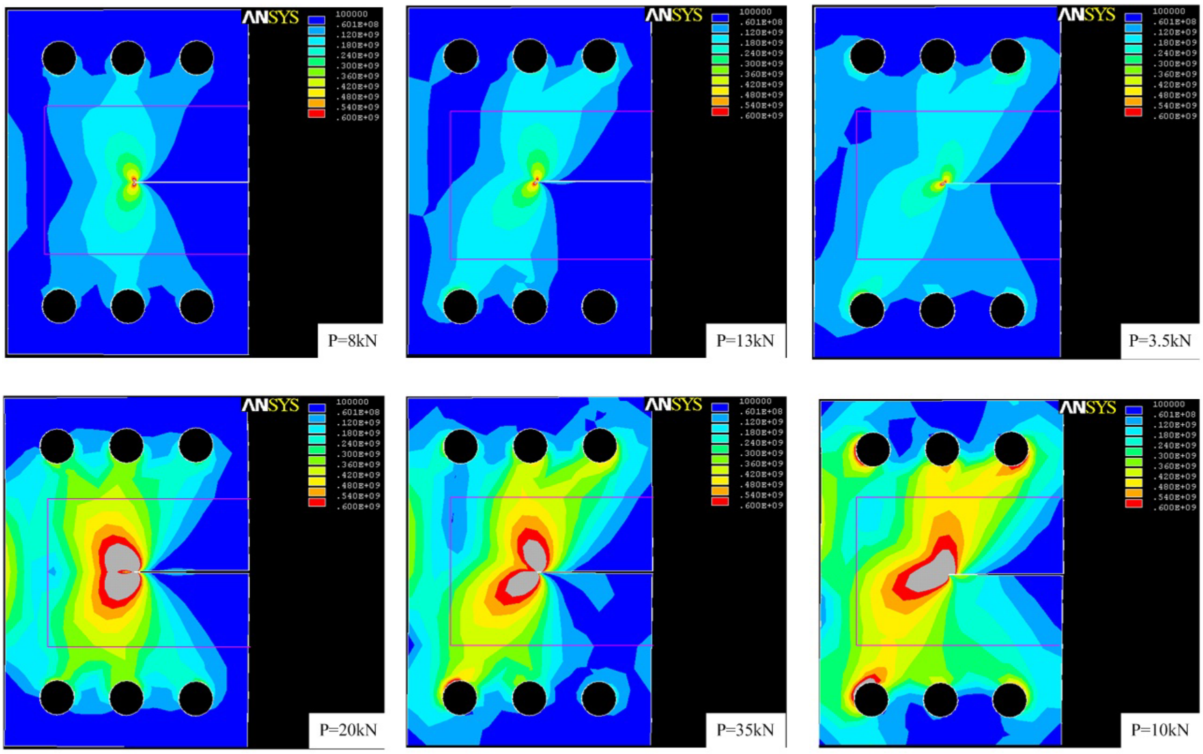

(a) b=4mm, 500℃, β=0° (b) b=7mm, 500℃, β=27° (c) b=2mm, 500℃,β=53°

Figure 6: ANSYS non-linear FE results (stress field and plastic zone on the front surface) at 500℃

considered. However, there are different exists in the second row, where the load is the maximum value before fracture in Figure 6 and the value under which the last clear moiré fringe is obtained in Figure 7. Based on Figures 6 and 7, numerical results apparently agree well with the experimental data. The displacement fields on the specimen surface by the moiré interferometry are invalid due to the existence of crack tip plasticity and out-plane deformation. As an amendment, the 3D FE simulation is a powerful auxiliary tool in the computation during late loading period, and the corresponding details will be described in future work. The hybrid experimental-numerical procedure [29] is believed to be an effective technique in the fracture analysis and prediction area.

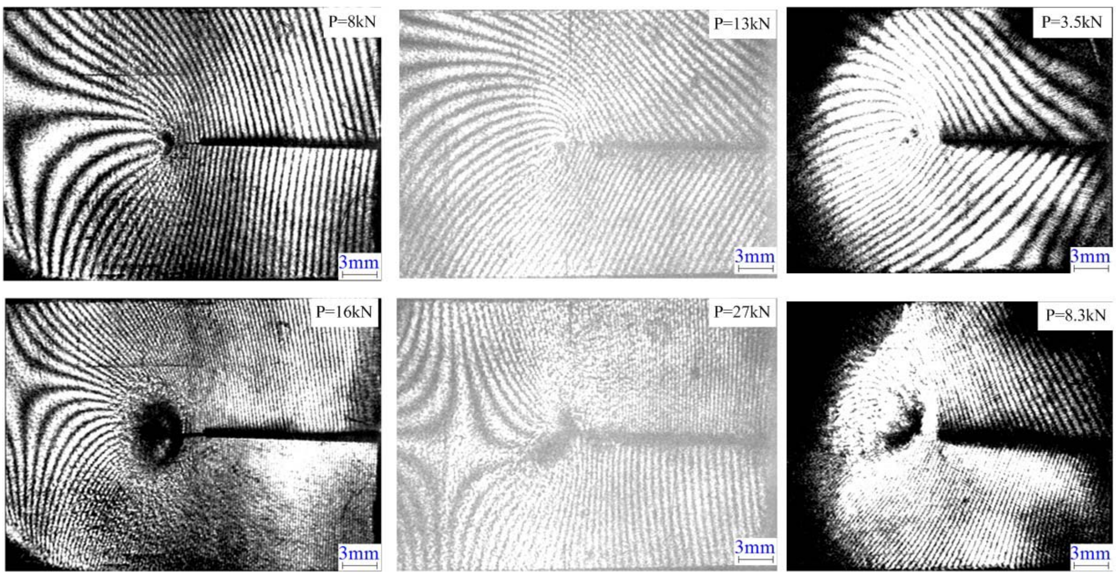

(a) b=4mm, 500℃, β=0° (b) b=7mm, 500℃, β=27° (c) b=2mm, 500℃, β=53°

Figure 7: Corresponding experimental results (displacement field and plastic zone on the front surface)

4. Conclusions

In the present paper, the newly developed fracture test equipment, techniques, and methodology based on moiré interferometry are presented in detail. Through real-time observation of fracture process around the crack tip and image acquisition of the moiré fringe at different loads, the magnitude of elastoplastic deformation and corresponding fracture parameters are extracted using the wave-front interference principle. In the test of TC11 finite specimen with through-thickness crack under mixed mode I-II loading, the duration from the beginning of loading to the ultimate fracture of specimen is relatively short, thereby causing difficulty in the determination of crack initiation moment. Moreover, no stable crack growth process is involved prior to the occurrence of unstable crack propagation. Concerning the common fracture mechanism on crack initiation, and the stable and unstable growth of metallic material, further investigation should be conducted to tell whether the size of crack tip plasticity zone on the surface can be adopted as a characteristic quantity of fracture. At the same time, the anomalous thickness effect of TC11 titanium alloy is reported, and the essence of this phenomenon is waiting to be uncovered.

Acknowledgements

The present work was supported by the National Natural Science Foundation of China (Grant nos. 61163048 and 11002066), the Aviation Science Foundation of China (Grant no. 2012ZF56027), and the Scientific Research Foundation of Key Laboratory of Nondestructive Testing, Ministry of Education (Grant no. ZD201129007).

References

[1] G.C. Sih, S. Tu, Z. Wang, Multiscaling Associated with structural and material integrity under elevated temperature. East China University of Science and Technology Press, Shanghai, 2006.

[2] Z. Wen, Z. Yue, Fracture behaviour of the compact tension specimens of nickel-based single crystal superalloys at high temperatures. Mat Sci Eng A, 456(2007) 189-201.

[3] S. Tu, F. Xuan, G. Wang, Recent progress in high temperature mechanical behavior of materials and structures. Chinese Journal of Solid Mechanics, 31(2010) 679-695.

[4] H. Shi, X. Ma, T. Yu, Some new progresses on the research of creep and fatigue behaviors of high temperature structural materials. Chinese Journal of Solid Mechanics, 31(2010) 696-715.

[5] S. Tu, F. Xuan, W. Wang, Some critical issues in creep and fracture assessment at high temperature. Acta Metallurgica Sinica, 45(2009) 781-787.

[6] F. Erdogan, Fracture mechanics. Int J Solids Struct, 37(2000) 171-183.

[7] A. Kotousov, Fracture in plates of finite thickness. Int J Solids Struct, 44 (2007) 8259-8273.

[8] W. Guo, Three-dimensional analyses of plastic constraint for through-thickness cracked bodies. Engng Fract Mech, 62 (1999) 383-407.

[9] T. Nakamura, D.M. Parks, Three-dimensional crack front fields in a thin ductile plate. J Mech Phys Solids, 38(1990) 787-812.

[10] X.M. Kong, N. Schluter, W. Dahl, Effect of triaxial stress on mixed-mode fracture. Engng Fract Mech, 52(1995) 379-388.

[11] H. Yuan, W. Brocks, Quantification of constraint effects in elastic-plastic crack front fields. J Mech Phys Solids, 46(1998) 219-241.

[12] Y.R. Arun, R. Narasimhan, An experimental investigation of constraint effects on mixed mode

fracture initiation in a ductile aluminirm alloy. Acta Mater, 47(1999) 1587-1596.
[13] Y. Kim, X.K. Zhu, Y.J. Chao, Quantification of constraint on elastic–plastic 3D crack front by the J–A2 three-term solution. Engng Fract Mech, 68 (2001) 895-914.
[14] S. Mahmoud, K. Lease, The effect of specimen thickness on the experimental characterization of critical crack-tip-opening angle on 2024-T351 alumimum alloy. Engng Fract Mech, 70(2003) 443-456.
[15] W. Guo, Elastoplastic three dimensional crack border field-I: Singular structure of the field. Engng Fract Mech, 46(1993) 93-104.
[16] W. Guo, Elastoplastic three dimensional crack border field-II: Asymptotic solution of the field. Engng Fract Mech, 46(1993) 105-113.
[17] W. Guo, Elastoplastic three dimensional crack border field-III: Fracture parameters. Engng Fract Mech, 51 (1995) 51-71.
[18] W. Guo, C. She, J. Zhao, B. Zhang, Advances in three-dimensional fracture mechanics. Key Engineering Materials, 312(2006) 27-34.
[19] H.R. Dong, W. Guo, Investigation on the experimental method for three-dimensional mixed mode fracture. Chinese Journal of Experimental Mechanics, 17(2002) 497-503.
[20] H.R. Dong, W. Guo, Mechanism Analysis of Thickness Effect on Mixed Mode I/II Fracture of LC4-CS Aluminum Alloy. Acta Metallurgica Sinica Letter, 3(2004) 255-262.
[21] D.J. Smith, T.D. Swankie, M.J. Pavier, M.C. Smith, The effect of specimen dimensions on mixed mode ductile fracture. Engng Fract Mech, 75(2008) 4394-4409.
[22] D.K. Tran, A.S. Kobayashi, K.W. White, Crack growth in alumina at high temperature. Engng Fract Mech, 68(2001) 149-161.
[23] B. Kang, X. Liu, C. Cisloiu, K. Chang, High temperature moiré interferometry investigation of creep crack growth of inconel 783 environment and β phase effects. Mat Sci Eng A, 347(2003) 205-213.
[24] X. Liu, B. Kang, W. Carpenter, E. Barbero, Investigation of the crack growth behavior of inconel 718 by high temperature moiré interferometry. J Mater Sci, 39(2004) 1967-1973.
[25] S. Zhang, W. Guo, H. Li, Y. Deng, Experimental investigation of three-dimensional mixed-mode fracture of a titanium alloy at room and elevated temperatures. Sci China Technol Sci, 54(2011) 2760-2767.
[26] H. Li, C.H. Yan, R.Z. Li, et al, Measuring elastic modulus and Poisson ratio for high-temperature materials by moiré inerferometry. Chinese J Mech Strength, 26(2004): 302-306.
[27] H. Li, S. Zhang, Y. Deng, Y. Wang, A removable system for in-plane displacement measuring based on moiré interferometry. Invention Patent, ZL200910115552.6.
[28] C.F. Shih, Small-scale yielding analysis of mixed mode plane strain crack problem. ASTM-STP 1974, 187-210.
[29] M.A. Sutton, M.L. Boone, F. Ma, J.D. Helm, A combined modeling-experimental study of the crack opening displacement fracture criterion for characterization of stable crack growth under mixed mode I/II loading in thin sheet materials. Engng Fract Mech, 66(2000) 171-185.